Journal of World Architecture, 2025, Volume 9, Issue 6
https://ojs.bbwpublisher.com/index.php/JWA
Online ISSN: 2208-3499
Print ISSN: 2208-3480

# Deformation and Failure Characteristics and Damage Characterization of Sandstone under Uniaxial Loading

**Jin Zhang[1], Qinming Xu[1], Mengyao Yu[2], Mengqi Wang[2]***

[1]Anhui Leiming Blasting Engineering Co., Ltd., Huaibei, Anhui, China
[2]Anhui University of Science and Technology, Huainan, Anhui, China

**Author to whom correspondence should be addressed.*



**Abstract:** To investigate the relationship between deformation, failure, and damage during the rock loading process, uniaxial compression tests were conducted on sandstone specimens. The characteristics of volumetric deformation and energy dissipation throughout the compression failure process were studied. Damage in the specimens was characterized using three physical parameters: crack volumetric strain, axial stiffness, and dissipated energy density. The results indicate that the loading process can be divided into five stages based on the crack volumetric strain. The instantaneous Poisson's ratio showed an increasing trend throughout all stages except the crack closure stage, with accelerated increase observed upon entering the unstable crack growth stage. Specimen dilatancy occurred during the stable crack growth stage. Radial cracks in their initial formation phase had minimal impact on the specimen's axial stiffness; a rapid decrease in axial stiffness only began during the unstable crack growth stage. Using axial stiffness and crack volumetric strain fails to adequately define damage during the crack closure and elastic stages. In contrast, characterizing specimen damage using dissipated energy density effectively reflects the damage evolution throughout the entire loading and failure process.

**Keywords:** Crack volumetric strain, Energy evolution, Stiffness degradation, Damage variable

**Online publication:** December 31, 2025

## 1. Introduction

The process of engineering excavation alters the stress state of rock masses, often resulting in varying degrees of damage to the surrounding rock [1]. The integrity of the surrounding rock is closely related to engineering safety, and reasonable damage characterization of rock is essential for evaluating rock mass stability and optimizing excavation design. After excavation, the triaxial stress in the rock mass near the free surface is released, approximating a uniaxial stress state. Due to mining-induced disturbance and abutment pressure, this part of the rock mass often experiences significant damage, making the study of its damage process highly important. Currently, numerous

scholars worldwide have proposed different methods for defining damage during the compressive failure process of rocks [2,3]. Wang *et al.* found that the circumferential strain rate during coal rock loading macroscopically reflects the initiation and propagation of internal cracks [4]. Mo *et al.* evaluated the damage variable using acoustic emission and plastic volumetric strain parameters, establishing a damage constitutive model based on this variable [5]. Guo *et al.* adopted plastic volumetric strain as the damage variable and developed a damage constitutive model for rocks using a normalization method [6]. Zhang *et al.* used energy dissipation density to define damage in granite [7]. Using the ultrasonic wave velocity method, Jin *et al.* defined the variation in rock damage variables through wave impedance [8]. Xiao *et al.* investigated the evolution of rock damage variables defined by acoustic emission counts under fatigue loading [9]. Li *et al.* defined a comprehensive damage variable based on the complementary relationship between the analytical expression of rock sample damage variables characterized by resistivity and those characterized by acoustic emission, deriving a damage evolution equation for typical rock samples [10].

It is evident that for rock damage under uniaxial loading, in addition to techniques such as acoustic emission, CT, nuclear magnetic resonance, and infrared radiation, damage in specimens can generally be characterized by physical parameters like plastic strain, crack volumetric strain, unloading modulus, and energy density [11,12]. This study is based on uniaxial compression tests of sandstone, investigating the mechanical parameters during its loading, deformation, and failure processes, and analyzing its energy evolution. Damage in the specimens is characterized from three perspectives: volumetric deformation, axial stiffness, and energy dissipation, with a comparison of different characterization methods.

## 2. Experimental overview

Large sandstone blocks collected from the mining face were transported to the laboratory and processed into cylindrical standard specimens with dimensions of $d \times h = 50 \times 100$ mm through coring, cutting, and grinding. The non-parallelism at both ends was controlled within 0.05 mm. The average density of the specimens was 2.34 $kg \cdot m^{-3}$, and the ultrasonic wave velocity was 3,120 m/s. Specimens with similar wave velocities were selected for the tests. The experiments were conducted on an RMT rock mechanics test system. To capture the post-peak behavior of the stress-strain curve, the tests employed displacement-controlled loading at a rate of 0.01 mm/s. Axial deformation was measured using an axial extensometer, while radial deformation was measured with a radial extensometer. The specimen loading setup is shown in **Figure 1**.

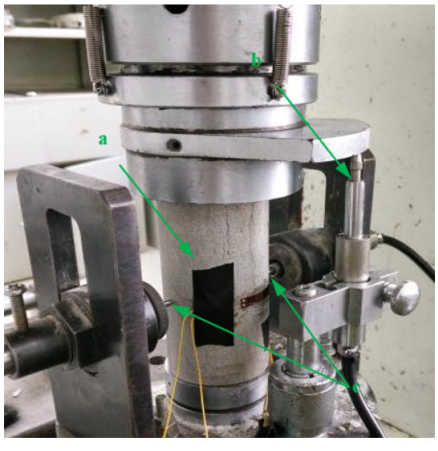


**Figure 1.** Uniaxial compression test of sandstone (a) Sandstone specimen (b) Axial extensometer (c) Radial extensometer.

# 3. Test results

## 3.1. Deformation characteristics of sandstone specimens

The stress-strain curve of the sandstone specimen under uniaxial load is shown in **Figure 2**. The volumetric strain of the specimen is obtained from **Equation (1)**:

$$\varepsilon_v=\varepsilon_a+2\varepsilon_r \tag{1}$$

Where $\varepsilon_v$ is the volumetric strain, $\varepsilon_a$ is the axial strain, $\varepsilon_r$ is the radial strain.

When the stress reached approximately 50% of the peak strength, the specimen began to exhibit dilatancy. Thereafter, with continued loading, the dilatancy accelerated. Compared to other types of hard brittle rocks, the sandstone specimen in this test showed more pronounced dilatancy after the peak stress. During the loading process of the rock specimen, internal microcracks gradually initiate and propagate. The crack volumetric strain is generally obtained indirectly, i.e., according to **Equation (2)**:

$$\varepsilon_c=\varepsilon_v-(1-2\mu)\sigma/E \tag{2}$$

Where, $\varepsilon_c$ is the crack volumetric strain; $\mu$ is Poisson's ratio, with a value of 0.26; $E$ is the elastic modulus, with a value of 10.01 GPa; Both $\mu$ and $E$ are obtained from the linear deformation segment of the axial stress-strain curve.

**Figure 2** shows the variation in crack volumetric strain of the specimen. Based on the curve characteristics, the loading process can be divided into five stages: crack closure stage (OA), linear elastic stage (AB), stable crack growth stage (BC), unstable crack growth stage (CD), and post-failure stage (DE). During the loading process, in the OA stage, microcracks and fissures are gradually compressed and closed, resulting in an increase in specimen stiffness, which is reflected in the upward concave shape of the curve. In the AB stage, the crack volume remains essentially constant, and the specimen exhibits favorable linear elastic behavior. During the BC stage, the crack deformation changes approximately linearly. In both the CD and DE stages, the crack volumetric strain increases rapidly. Throughout the entire loading and failure process, the crack volumetric strain generated during the crack closure stage is approximately $0.10\times10^{-2}$, while the crack volumetric strain produced during the crack growth stage (BE stage) is $1.48\times10^{-2}$. It is important to note that although the BC segment appears linear on the axial stress-strain curve, the crack volumetric strain continuously increases within this stage. This is because the radial deformation does not follow a linear elastic pattern, suggesting that the new cracks generated in this stage are primarily vertical. This observation is corroborated by the final failure mode of the specimen, which is predominantly splitting failure, as shown in **Figure 3**.

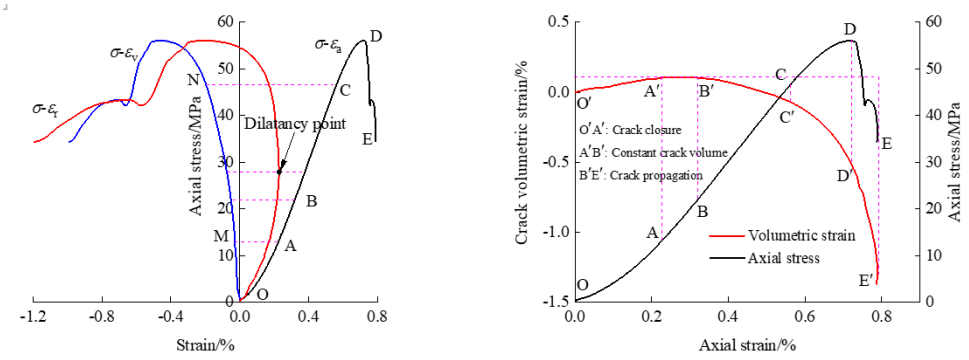


**Figure 2.** Uniaxial compression deformation curves of sandstone specimen (Left) Stress-strain curve (Right) Crack volumetric strain.

**Figure 3.** Splitting failure mode of specimen.

Moreover, as observed in **Figure 4**, the Poisson's ratio within segment AC increases approximately linearly with axial strain, indicating that the radial strain accelerates at a rate of  (where $k$ is the slope of segment FH), corresponding to segment MN in the a-b stage of **Figure 2**. The instantaneous Poisson's ratio of the specimen in **Figure 3** remains relatively low during segment OA, suggesting that axial deformation dominates in this loading stage. However, the instantaneous Poisson's ratio increases at an accelerated rate during segment CD, reflecting an unstable state of radial deformation.

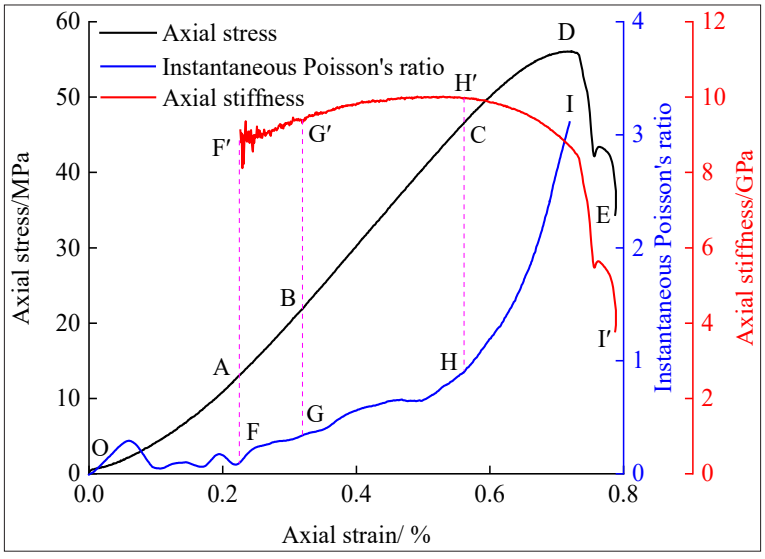


**Figure 4.** Variation in instantaneous Poisson's ratio and axial stiffness of sandstone specimen.

The axial stiffness in segment OA is lower than that in segment AB due to the compaction of pores and fissures and the corresponding nonlinear deformation under relatively low load. Therefore, **Figure 4** only presents the variation in axial stiffness starting from the elastic segment. It can be observed that the maximum value of the axial stiffness variation curve occurs in the stable crack growth stage rather than the linear elastic stage. As analyzed earlier, radial cracks begin to propagate from point B, yet the axial direction of the specimen appears to

remain in a "compaction stage," indicating that radial cracks in their initial formation stage do not substantially affect the axial stiffness of the specimen. It is only after entering the unstable crack growth stage that the axial stiffness of the specimen begins to decrease. At this point, the Poisson's ratio approaches 1, and the axial stiffness diminishes at an even faster rate in the post-failure stage.

## 3.2. Energy dissipation characteristics

The failure of the specimen is a result driven by energy. Analyzing the deformation and failure process of sandstone specimens from an energy perspective is of significant importance. During the loading process, the energy input to the specimen by the testing machine is partially stored within the specimen as elastic energy, while the remainder is dissipated in forms such as plastic deformation energy, acoustic energy, and thermal energy. The input energy to the specimen is represented by the area enclosed between the axial stress-strain curve and the strain axis, which can be obtained through integration. By considering the matrix part of the specimen as an elastic body, the elastic energy during the loading process can also be determined, thereby allowing the calculation of the dissipated energy. Relevant energy calculations are provided in **Equations (3)** to **(5)**:

$$u_i = \int \sigma d\varepsilon \tag{3}$$

$$u_i = u_e + u_d \tag{4}$$

$$u_e = \sigma^2 / 2E \tag{5}$$

Where $u_i$ is the input energy density; $u_e$ is the elastic energy density; $u_d$ is the dissipated energy density.

The calculated variations of the three energy densities with axial strain are shown in **Figure 5**. Among these energy densities, the dissipated energy density reflects the energy loss during the deformation and failure process of the specimen and indirectly indicates the extent of damage evolution. The curve of dissipated energy density in the figure can be divided into two stages, corresponding to segments OC and CE of the stress-strain curve, respectively. In segment OC, the dissipated energy density increases slowly. After point C, i.e., upon entering the unstable crack growth stage, the rate of dissipated energy generation gradually accelerates. Concurrently, the specimen's capacity to store elastic energy begins to diminish, leading to a slowdown in the rate of increase of elastic energy density starting from point C, and even a sharp decline in the post-failure stage.

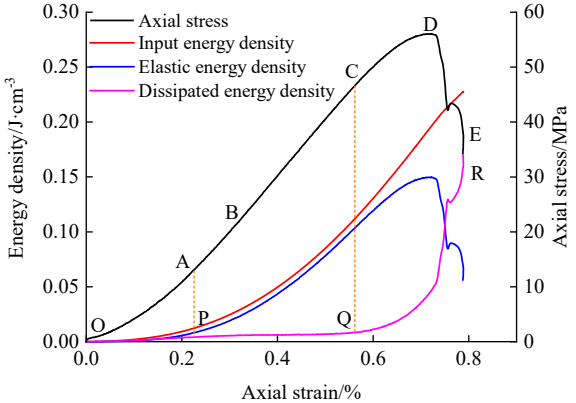


**Figure 5.** Energy density variation during specimen loading.

## 4. Damage characterization of sandstone

The preceding analysis demonstrates that crack volumetric strain, energy dissipation, and axial stiffness are closely related to the deformation and failure process of the specimen. Consequently, the damage in the specimen can be characterized using crack volumetric strain and dissipated energy density. Regarding crack volumetric deformation, the crack deformation generated during the crack closure stage is primarily attributable to processes such as rock mass excavation, rock transportation, and laboratory processing, and has a minimal impact on the overall specimen. Therefore, when normalizing the damage characterization based on crack volumetric strain, it is appropriate to calculate from the crack initiation point. The calculation formula is as follows:

$$D_c=\varepsilon_c/\varepsilon_c^t \tag{6}$$

Where $\varepsilon_c$ is the crack volumetric strain at any given load level (after point B); $\varepsilon_c^t$ failure is the cumulative crack volumetric strain at specimen failure.

The damage characterized by dissipated energy density is given by **Equation (7)**:

$$D_d=u_d/u_d^t \tag{7}$$

Where $u_d$ is the dissipated energy density at any given time; $u_d^t$ is the cumulative dissipated energy density at specimen failure.

The degradation of axial stiffness indicates that damage has occurred in the specimen. Therefore, the damage can be characterized by the reduction in axial stiffness:

$$D_s=\frac{S_{max}-S}{\Delta S} \tag{8}$$

Where $S_{max}$ is the maximum axial stiffness, with a value of 10.01 GPa; $S$ is the axial stiffness at any given loading point; $\Delta S$ is the cumulative reduction in stiffness at specimen failure, with a value of 6.23 GPa.

Based on **Equations (6)** to **(8)**, the damage variables of the specimen characterized by the three methods are shown in **Figure 6**. Overall, the variation trends of the three damage variables are consistent, but certain differences exist. When characterized using stiffness degradation and crack volumetric strain, the damage throughout the entire loading process cannot be fully defined, whereas characterization using dissipated energy density enables the determination of damage across the full loading process. In the BC stage, the damage variables remain largely unchanged when characterized by dissipated energy density and axial stiffness, while characterization by crack volumetric strain shows an approximately linear increase. After entering the unstable crack growth stage, all three damage variables exhibit an accelerating upward trend.

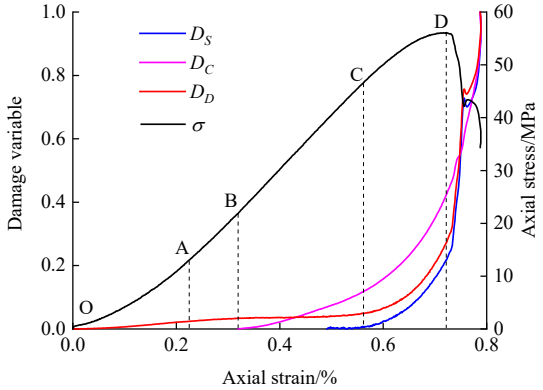


**Figure 6.** Damage variables defined by three characterization methods.

In practice, the characterization based on stiffness degradation is measured from the perspective of axial deformation characteristics of the specimen. However, it fails to account for the increase in stiffness during the early loading stage, exhibiting certain limitations. In contrast, crack volumetric strain considers both axial and radial deformations, making it a more comprehensive method than the former. Since radial cracks in their initial stage have minimal impact on axial stiffness, the characterization based on crack volumetric strain covers a relatively broader range. Nevertheless, using these two methods to characterize damage during the initial loading stage may result in negative values, which is referred to as "negative damage" [13]. Characterization using dissipated energy density, however, can avoid the occurrence of "negative damage." Moreover, it reveals that the damage during the initial loading stage is significantly smaller than the damage generated upon entering the unstable crack growth stage, which aligns with reality. This is because the dissipated energy during the crack closure stage primarily originates from the compaction of micro-pores and fissures, as well as friction along fissure surfaces within the specimen. The damage formed in this process is considerably smaller compared to the damage caused by crack nucleation and propagation in the later stages of loading.

In the post-failure stage, external work (loading by the testing machine) noticeably slows down, yet the damage rate of the specimen increases. This phenomenon can be reasonably explained from the perspective of energy dissipation. During the loading and failure process of the specimen, cracks initiate, propagate, and coalesce, eventually forming macroscopic failure surfaces. Before the peak stress, internal cracks gradually develop, and elastic energy is partially released. However, as no significant failure surfaces have formed, the rate of elastic energy release remains lower than the rate of accumulation, resulting in a continued increase in elastic energy before the peak stress. After the peak stress, macroscopic fracture surfaces extensively develop. Although external energy continues to be input, the rate of elastic energy release exceeds the rate of storage. Consequently, the elastic energy accumulated before the peak stress is continuously released and transformed into other forms of energy, such as plastic energy, damage energy, radiant energy, and kinetic energy, leading to intensified damage and driving the specimen toward a stable state.

## 5. Conclusion

The linear elastic stage of the specimen is relative. The instantaneous Poisson's ratio exhibits a continuous increasing trend after entering the linear elastic stage and accelerates upon reaching the unstable crack growth stage, during which the axial stiffness also degrades at an accelerating rate. Dilatancy of the specimen occurs during the stable crack growth stage. The crack initiation point in the specimen occurs before the onset of stiffness degradation. Crack initiation is predominantly radial, and the initial formation of cracks has a minimal impact on the axial stiffness. Both the crack volumetric strain and the dissipated energy density increase at an accelerated rate after entering the unstable crack growth stage. Damage during the crack closure and elastic stages cannot be adequately defined using axial stiffness or crack volumetric strain. Furthermore, these two damage variables exhibit differences during the stable crack growth stage. In contrast, characterizing specimen damage using dissipated energy density effectively reflects the damage evolution throughout the entire loading process.

## Disclosure statement

The authors declare no conflict of interest.

## References


[1] Niu S, Jing H, Yang X, et al., 2012, Experimental Study of Strength Degradation Law of Surrounding Rock in Fractured Zone of Deep Roadway. Chinese Journal of Rock Mechanics and Engineering, 31(8): 1587–1596.

[2] Kim J, Lee K, Cho W, et al., 2015, A Comparative Evaluation of Stress-Strain and Acoustic Emission Methods for Quantitative Damage Assessments of Brittle Rock. Rock Mechanics and Rock Engineering, 48(2): 495–508.

[3] Xie H, Dong Y, 1997, Research on Plastic Modulus Method for Classical Damage Mechanical Definition. Mechanical and Practice, 19(2): 1–5.

[4] Wang C, Yang X, Guo W, et al., 2015, Statistical Damage Constitutive Model for Coal and Rock Uniaxial Loading. Coal Mine Safety, 46(11): 10–13.

[5] Mo Y, Zeng Y, Li J, et al., 2013, Multiparameter Constitutive Model of Rock Damage under Uniaxial Loading. Chinese Journal of Underground Space and Engineering, 9(3): 477–481.

[6] Guo Z, Liu X, Liu B, et al., 2010, Experimental Study of Deformation Characteristics of Rock Damage based Plastic Volume Strain. Journal of Experimental Mechanics, 25(3): 293–298.

[7] Zhang Z, Zhu J, Wang B, et al., 2018, The Damage and Shear Dilation Property Evolution based on Energy Dissipation Mechanism of Gneissic Granite. Chinese Journal of Rock Mechanics and Engineering, 37(s1): 3441–3448.

[8] Jin J, Zhong H, Wu Y, et al., 2013, Method Selection for Defining Damage Variable of Rock Subjected to Static Loadings and Cyclic Impacts. Nonferrous Metals Science and Engineering, 4(4): 85–90.

[9] Xiao J, Ding D, Jiang F, et al., 2010, Fatigue Damage Variable and Evolution of Rock Subjected to Cyclic Loading. International Journal of Rock Mechanics and Mining Sciences, 2010(47): 461–468.

[10] Li S, Xu X, Liu Z, et al., 2014, Electrical Resistivity and Acoustic Emission Response Characteristics and Damage Evolution of Sandstone during Whole Process of Uniaxial Compression. Chinese Journal of Rock Mechanics and Engineering, 33(1): 14–23.

[11] Li J, Zhou K, Zhang Y, et al., 2012, Experimental Study of Rock Porous Structure Damage Characteristics under Condition of Freezing-Thawing Cycles based on Nuclear Magnetic Resonance Technique. Chinese Journal of Rock Mechanics and Engineering, 31(6): 1208–1214.

[12] Jin P, Wang E, Liu X, et al., 2013, Damage Evolution Law of Coal-Rock under Uniaxial Compression based on the Electromagnetic Radiation Characteristics. International Journal of Mining Science and Technology, 23(2): 213–219.

[13] Zhang Q, Yang G, Ren J, 2003, New Study of Damage Variable and Constitutive Equation of Rock. Chinese Journal of Rock Mechanics and Engineering, 22(1): 30–34.